

# An expandable kinetic Monte Carlo platform for modelling electron transport through chiral molecules

Silvia Giménez-Santamarina<sup>\*1</sup>, Andrés Mora Martínez<sup>1</sup>, Gérliz M. Gutiérrez-Finol<sup>1</sup> and Alejandro Gaita-Ariño<sup>\*1</sup>

Address: <sup>1</sup>Instituto de Ciencia Molecular (ICMol), Universitat de València, Paterna, Spain

Email: Silvia Giménez-Santamarina - silvia.m.gimenez@uv.es; Alejandro Gaita-Ariño - gaita@uv.es

<sup>\*</sup> Corresponding author

## Abstract

Molecular chirality interacting in a non-negligible manner with the spin angular momentum of subatomic particles, mainly electrons or photons, is the cause of a variety of spin-dependent filtering effects in quantum transport. Among them, spin-selective transport at room temperature is clearly one of the most promising properties in the quest for functional spintronic devices. In this context, two main effects have been experimentally investigated in the past 25 years and have attracted significant interest within the community: the so-called Electronic Magnetochiral Anisotropy (eMChA) and Chirality Induced Spin Selectivity (CISS). Despite extensive research, there is still a lack of consensus in the modeling of their microscopic mechanisms. As a consequence, it remains unclear whether the two are truly distinct or if they originate from a common physical cause. With the long-term goal of modelling the main different theories and to test them against the available experimental evidence, we programmed the core of an efficient kinetic Monte Carlo code. The current code models electron transport under an external voltage, distinguishes between  $\alpha$  and  $\beta$  spin currents, and parametrizes molecules by their intrinsic electron mobility and the effective coupling between electron movement, spin and chirality. The code allows obtaining spin filtering values arising from the

effective coupling between these three. We obtain an effect that vanishes at low voltages, with the asymmetry between positive and negative voltages typically found in electrical magnetochiral anisotropy experiments.

## Keywords

Electrical magnetochiral anisotropy; kinetic Monte Carlo; spintronics

## Introduction

### Interaction between chirality and spin transport

Spintronics exploits the electron's spin degree of freedom to transport, process, and store information, offering prospects for low-power and high-speed devices beyond conventional charge-based electronics. However, traditional spintronic architectures rely on ferromagnetic materials and strong magnetic fields, which limits scalability and integration with molecular, organic, and biological systems. These limitations have motivated growing interest in non-magnetic routes to spin control, particularly mechanisms that directly couple charge transport to spin polarization under ambient conditions. [1,2]

Chiral molecular systems, those characterized by the absence of mirror and inversion symmetries, exhibit singular electrical and optical properties arising from their interaction with the quantum mechanical degrees of freedom of matter, including electronic structure, spin, and optical activity. In this context, processable chiral nanostructures are exceptional platforms for exploiting electrical effects that arise from symmetry-breaking interactions between electronic motion, charge and spin. In particular, it has been demonstrated that an electrical current of initially unpolarized electrons traversing a chiral material can become spin-polarized, with preferential charge and spin transport depending on both the handedness of the chiral structure and the direction of electron motion.

Such spin-selective behavior has been observed across a wide range of materials and exper-

imental conditions, including self-assembled monolayers of DNA, peptides, helicenes, polymers, and hybrid chiral nanostructures. Measurements using magnetic conductive atomic force microscopy, photoemission, magnetoresistance, and electrochemical techniques consistently reveal sizeable spin polarizations at room temperature, despite the absence of ferromagnetic components within the chiral layers themselves. [1-3]

## **Theoretical frameworks: eMChA vs CISS**

These experimental observations are commonly discussed within two closely related frameworks: Chirality Induced Spin Selectivity (CISS) and electronic magnetochiral anisotropy (eMChA). Both effects appear to originate from the coupling between electron spin and a chiral electrostatic potential, yet they are characterized by distinct experimental signatures and measurement protocols.

Electronic magnetochiral anisotropy refers to a differential magnetoresistance that depends on the handedness of the chiral structure and on the relative orientation of the electrical current and an external magnetic field. Reversing either the current direction or the magnetic field leads to asymmetric conductance responses. [4-7] In contrast, CISS is defined as the difference in transport efficiency for spin-up and spin-down electrons along a chiral conductor, even in the absence of an applied magnetic field, with the effect depending on molecular handedness and charge transport direction. [8]

A similar distinction arises in optical analogues of magnetochiral effects, where magnetochiral anisotropy requires an external magnetic field, while CISS is often claimed to be an intrinsic property of chiral materials. [8] However, directly measuring CISS remains experimentally challenging, as it would require highly efficient spin-resolved detection. As a result, many experiments probe CISS indirectly by using external magnetic fields or ferromagnetic contacts to polarize the incoming electrons and comparing transport signals for opposite spin orientations. [8]

Despite extensive experimental and theoretical efforts, a unified and straightforward mi-

croscopic explanation for either CISS or eMChA remains elusive. Numerous theoretical models have been proposed, invoking mechanisms ranging from enhanced spin-orbit coupling and quantum coherence effects to many-body interactions, decoherence, and vibronic coupling. The complex interplay between geometry, symmetry breaking, electronic spin, and nonequilibrium dissipation makes it unclear whether CISS and eMChA should be regarded as distinct phenomena or as different manifestations of a common underlying chiral spin-transport mechanism operating in different regimes.

## **Microscopic, frugal, expandable modelling**

Addressing these open questions calls for controlled modeling frameworks capable of systematically testing microscopic assumptions, varying physical parameters, and connecting them directly to experimentally accessible observables. In this work, we focus on developing a microscopic phenomenological model based on kinetic Monte Carlo (kMC) methods to describe charge and spin transport under an applied electric potential in chiral molecular structures, with the long-term goal of providing insight into the physico-chemical mechanisms governing both CISS and eMChA.

Kinetic Monte Carlo approaches naturally capture nonequilibrium, stochastic transport processes on discrete networks while remaining computationally efficient over experimentally relevant time and length scales. Previous applications of similar kMC methodologies have successfully reproduced key experimental features in diverse contexts, including magnetic memory effects in nanomagnets [9] and memristive behavior in solid-state ion conduction. [10]

Here, we present the core of an efficient kinetic Monte Carlo model that explicitly incorporates spin degrees of freedom, molecular chirality, and applied bias, and is designed to address eMChA and, in future extensions, CISS. In this initial implementation, we demonstrate the minimal functionality of the model and illustrate how effective couplings between charge motion, spin, and chirality give rise to spin-dependent transport signatures. The modular structure of the code is intended to facilitate systematic incorporation of existing and emerging theoretical

mechanisms and to enable frugal reuse of experimental data to benchmark individual models or combinations thereof against the growing body of experimental evidence.

## Results and Discussion

### Basic electron transport modelling and relation with the CupFlow code

The present implementation models electron transport in an ensemble of identical molecular strands, each hosting a single conducting electron, under the influence of an external voltage applied by electrodes at the two ends of the molecules. The applied voltage  $V$  and the molecular length  $l$  are treated as external parameters. Together with the electron charge  $e$ , they define a total electrostatic energy drop across each molecule,  $E = V \cdot e$ . A linear potential profile is assumed along the molecular backbone, such that an electron displacement over a distance  $\Delta_l$  corresponds to an energy change:

$$\Delta E = \frac{\Delta_l}{l} V e \quad (1)$$

The intrinsic electron mobility of the molecules at room temperature is parametrized by a characteristic hopping time  $\tau$ , with the diffusion coefficient  $D$  being proportional to the inverse of the time  $1/\tau$ :

$$D \propto 1/\tau \quad (2)$$

A straightforward extension of the model consists in expressing  $\tau$  in terms of an effective energy barrier  $U_{\text{eff}}$ , an attempt time  $\tau_0$ , and the temperature  $T$ , for instance through an Orbach-type activated process:

$$\tau = \tau_0 \exp\left(-\frac{U_{\text{eff}}}{T}\right). \quad (3)$$

Within these assumptions, the kinetic Monte Carlo algorithm interrogates, at each time step,

whether each electron undergoes a hopping event, following the same strategy previously validated for magnetic relaxation processes in the STOSS and DAISY codes. [9,11] When a hopping event occurs, the direction of electron motion is determined probabilistically, with transition probabilities proportional to the ratio of Boltzmann populations evaluated at the working temperature  $T$  and the corresponding energy difference  $\Delta E$ , in direct analogy with the procedure employed in the CupFlow code for ion transport. [10] This approach represents a natural extension of the methodology originally developed for spin relaxation in STOSS to charge transport under an applied electric field.

A key difference with respect to CupFlow is that the latter was designed to model ion migration within solid-state devices, where continuous electrical current cannot be directly defined and only charge accumulation near the electrodes can be monitored. In the present implementation, we extend the framework to explicitly allow for steady-state current flow. Specifically, when an electron exits the system through the right end of the molecule, it is considered drained, reintroduced at the left end to conserve the total number of charge carriers, and a corresponding event is recorded. Conversely, when an electron exits through the left end, it is reintroduced at the right end and a sourced event is registered. The net electron current is defined as the difference between sourced and drained events, normalized by the total simulation time.

## **Validation: recovering Ohm's law and resistivity equations**

The stochastic transport model introduced above does not explicitly incorporate dissipative mechanisms, nor does it enforce macroscopic circuit relations by construction. In particular, neither Ohm's law, which states that the electrical current is proportional to the applied voltage, nor the standard resistivity relationship, according to which the electrical resistance scales linearly with the length of the conductor and inversely with its cross-sectional area, is imposed at any stage of the simulation. These relations are therefore not built into the model but must instead emerge from the underlying microscopic dynamics. Establishing that this behavior

emerges naturally from the model constitutes an essential validation step before addressing spin- and chirality-dependent transport effects.

Within the model, charge transport proceeds through stochastic forward and backward electron hops along the molecular backbone, with a slight bias introduced by the applied electric field. This bias favors motion along the field direction and depends on the total voltage drop across the molecule as well as on its length. Despite the simplicity of this mechanism, the resulting steady-state current displays a linear dependence on the applied bias and decreases with increasing molecular length, reproducing the expected macroscopic behavior associated with Ohmic transport.

The magnitude of the current also scales with the number of parallel molecular strands contributing to transport, which plays the role of an effective cross-sectional area. At the microscopic level, the material resistivity is controlled by the characteristic time associated with individual hopping events, or equivalently by the effective charge diffusivity. When this hopping time is modeled as a thermally activated process, the resulting conductivity exhibits an exponential dependence on temperature, as commonly observed in semiconducting systems. In this formulation, the attempt time reflects the choice of the elementary spatial discretization used to represent the molecular structure.

Taken together, these observations demonstrate that standard resistive transport behavior emerges naturally from the stochastic electron dynamics implemented in the model, even in the absence of explicitly imposed circuit-level relations.

## Introducing spin

In the simulation, the dynamical state of the system is represented by matrices that store the position of each electron along its molecular strand at every time step. In addition to the spatial degree of freedom, each electron is assigned a fixed spin label, allowing spin-resolved transport to be explicitly tracked throughout the simulation.

Electron transport is simulated independently for two spin channels, denoted here as  $\alpha$  and

$\beta$ . These labels correspond to the two possible projections of the electron spin along a fixed quantization axis, with  $\alpha$  spins defined as parallel and  $\beta$  spins as antiparallel to that axis. The choice of quantization axis is fixed throughout the simulation and serves solely as a reference for defining spin-dependent transport channels; it does not imply the presence of a dynamically evolving magnetic field or coherent spin dynamics.

For each spin channel, hopping events that carry electrons across the left and right boundaries of the molecular strand are recorded separately. These boundary-crossing events provide an operational definition of spin-resolved electrical currents, defined as the net imbalance between crossings at the two ends over the duration of the simulation. Comparing the resulting currents for the two spin channels directly quantifies the spin selectivity of the transport process.

In the present implementation, the spin degree of freedom influences transport only through spin-dependent hopping probabilities, while spin-flip processes are neglected. This corresponds to the assumption that spin relaxation occurs on time scales longer than those governing charge transport, or that its effects can be effectively absorbed into phenomenological transport parameters. Explicitly keeping track of spin states nevertheless renders the framework readily extensible: stochastic spin dynamics or coupling to external fields can be incorporated in future versions of the model if required by the relevant physical regime. For instance, including spin-flip events.

## Recovering eMChA

Spin-dependent transport effects are introduced in the model by augmenting the energy difference associated with an elementary hopping event,  $\Delta_E$ , with a term whose sign depends on the combined action of spin, chirality, and transport direction. Specifically, the sign factor is taken as  $(-1)^{s \cdot c \cdot v}$ , where the spin variable  $s$  is defined as  $+1$  for electrons with  $\alpha$  spins and  $-1$  for electrons with  $\beta$  spins, the chirality index  $c$  is  $+1$  for left-handed and  $-1$  for right-handed molecular helices, and the velocity index  $v$  distinguishes motion parallel ( $+1$ ) or antiparallel ( $-1$ ) to

the chosen spin quantization axis. This construction captures the symmetry requirements expected for magnetochiral transport phenomena, where the transport response changes sign under reversal of any one of these three quantities.

To model electric magnetochiral anisotropy, we assume that the relevant spin-dependent contribution originates from spin-orbit coupling to the magnetic field generated by charge motion along a chiral trajectory. Importantly, an electron undergoing random, back-and-forth hopping over short distances does not generate a net magnetic field that can couple to its own spin. This situation corresponds to the low-voltage, diffusion-dominated regime of transport, where the electric current is negligible and the eMChA signal is therefore expected to vanish. This behavior is consistent with experimental observations showing the suppression of magnetochiral effects in the linear-response limit.

In contrast, when transport is driven by an applied voltage, electrons acquire a net directional motion along the molecular helix. In this regime, the circulating charge density generates a magnetic field that can act on the same electronic states, enabling a coupling between orbital motion and spin. One possible way to model this effect would be to explicitly track the trajectory history of each electron and activate the spin-orbit coupling term only after a threshold number of consecutive hops in the same direction, mimicking the buildup of a persistent current. This approach is conceptually similar to the Hamiltonian proposed by Fransson, where spin-orbit coupling connects next-nearest-neighbor sites, while nearest-neighbor hopping remains spin independent.[12]

However, explicitly storing and processing trajectory histories would significantly increase the computational complexity of the simulation. Instead, we adopt a more compact phenomenological approach that exploits a key property of the present model: the net electrical current generated by an applied voltage scales as a hyperbolic tangent function of the voltage. Since the magnetic field associated with the orbital motion is itself proportional to the current, we model the effective spin-orbit contribution to the magnetochiral energy term as being modulated by a  $\tanh(V)$  dependence. This choice ensures that the eMChA contribution vanishes at

zero voltage, grows linearly at small voltages where the current is proportional to the electric field, and saturates at large voltages when the current reaches its maximum value.

The resulting behavior of the model reproduces the key qualitative features expected for electric magnetochiral anisotropy, as illustrated in Fig. 1. At low voltages, electrons with  $\alpha$  and  $\beta$  spin projections respond identically to the applied bias, resulting in a linear current-voltage characteristic and a vanishing eMChA signal. At higher voltages, the spin-dependent asymmetry becomes apparent: for a positive magnetochiral coupling,  $\beta$  electrons exhibit a lower resistance at positive bias and a higher resistance at negative bias, while  $\alpha$  electrons show the opposite behavior. At sufficiently large voltages, the transport for both spin channels converges toward the same saturation current, reflecting the finite upper bound imposed by the hopping dynamics.

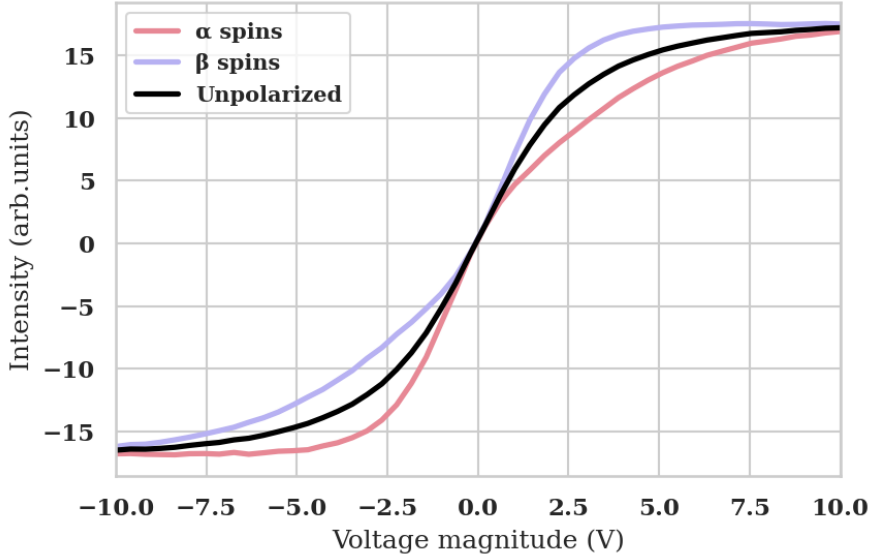


**Figure 1:** Current-voltage curve obtained from the kinetic Monte Carlo simulation for  $\alpha$  (red curve) and  $\beta$  (purple curve) spin channels, together with the corresponding unpolarized current. The results are shown for a system comprising  $N = 5500$  electrons distributed over identical molecular strands, a dimensionless diffusion coefficient  $D = 0.1$  controlling the overall hopping rate, and a phenomenological spin-chirality coupling strength  $Q_{\text{Ciss}} = 0.4$  that introduces spin-dependent asymmetry in the hopping probabilities. The currents are reported in arbitrary units and exhibit a nonlinear voltage dependence with spin-resolved asymmetry characteristic of electric magnetochiral anisotropy.

A final remark concerns the role of the external magnetic field. In the present simulator, an explicit magnetic-field dependence does not need to be introduced, as the expected lin-

ear behavior emerges naturally from the underlying assumptions. This can be understood by considering two limiting regimes: the high-field, low-temperature limit and the low-field, high-temperature limit.

In the high-field limit, the Zeeman energy dominates over thermal fluctuations, and the electronic spins become fully aligned with the external magnetic field. This situation effectively corresponds to the conditions realized in many CISS experiments, where spin-polarized currents are typically generated using ferromagnetic or otherwise spin-selective electrodes rather than by applying a strong external magnetic field.

By contrast, eMChA experiments are commonly performed in the low-field regime, where the Zeeman energy remains much smaller than the thermal energy. In this limit, the net spin polarization is weak and varies linearly with the applied magnetic field. When transport occurs through a chiral conductor that exhibits different resistances for opposite spin orientations, the contributions from the two spin channels largely cancel for weakly polarized currents. The residual signal is therefore proportional to the small spin imbalance.

Since this spin excess itself scales linearly with the magnetic field in the low-field regime, the resulting electric magnetochiral anisotropy signal also exhibits a linear dependence on  $B$ . This argument explains why an explicit magnetic-field term is not required in the simulation to recover the experimentally observed magnetic-field scaling of the eMChA effect.

## Perspectives

The current version of the model presented here covers yet a basic functionality. However, it already reproduces both the spinless equations of electric resistors and the qualitative shape of the eMChA dependence on voltage and on magnetic field. Its potential is interesting, since it is inherently expandable, allowing to build on existing works without compromising its frugal character. For instance, note that our kMC code DAISY [9] is able to recover experimental ac phenomena, such as in-phase and out-of-phase susceptibility in single-molecule magnets. In turn, the related CupFlow can reproduce experiments which alternate increasing and decreas-

ing voltage in a setup that registers charge accumulation rather than charge flow.[10] Thus, one could easily combine parts from the three codes to explore the modelling of dielectric magneto-chiral anisotropy, the latest member of the magnetochiral anisotropy phenomena. [13]

## Methods

### Current, voltage and saturation

Before considering any interaction with chirality, a system with charged carriers under an applied voltage  $V$  exhibits an intrinsic asymmetry between forward (rightward) and backward (leftward) transition probabilities. Assuming a Boltzmann distribution for the transition rates, the probability for an electron to move in the direction of the electric field ( $P_+$ ) or against it ( $P_-$ ) can be written as:

$$P_+ = \frac{e^{-\beta qV}}{e^{-\beta qV} + e^{\beta qV}}, \quad P_- = \frac{e^{\beta qV}}{e^{-\beta qV} + e^{\beta qV}}, \quad (4)$$

where  $\beta = 1/(k_B T)$  is the inverse thermal energy,  $q$  is the electron charge, and  $T$  is the temperature.

The net directional imbalance, and therefore the net current, is proportional to the difference in these probabilities:

$$I \propto |\Delta P| = |P_+ - P_-| = \tanh\left(\frac{qV}{k_B T}\right). \quad (5)$$

This result shows a hyperbolic tangent profile, with the probability imbalance increasing linearly with voltage at low bias and saturating at high bias due to thermal broadening.

### Helicity and spin-orbit-coupling

Based on this outcome, the emergence of spin-dependent transport in chiral systems can be qualitatively understood as a two-step process. Firstly, an applied voltage  $V$  induces a net cur-

rent due to the asymmetry between forward and backward transition probabilities. Secondly, this current generates a magnetic field via Ampère's law.

This magnetic field points perpendicular to the direction of charge transport and to the chiral axis of the molecule. As a result, electrons moving through the chiral medium experience an effective magnetic field whose magnitude is proportional to the current, and hence to  $\tanh(qV/k_B T)$ . This magnetic field couples to the electron spin via spin-orbit coupling (SOC), producing a spin-dependent energy correction.

Therefore, the total energy variation associated with a transition should include not only the purely electric contribution,  $qV$ , but also a spin-dependent term of the form  $\mu \cdot B$ , where  $\mu$  is the electron magnetic moment and  $B$  is the effective magnetic field generated by the current. Phenomenologically, we model this additional term as:

$$E_{\text{eMChA}} = \Gamma \cdot s \cdot \tanh\left(\frac{qV}{k_B T}\right), \quad (6)$$

where  $\Gamma$  is a parameter capturing the maximum magnitude of the eMChA-induced spin-orbit energy shift and  $s = \pm 1$  denotes the electron spin orientation. This contribution represents the effective spin-dependent potential arising from the SOC mediated by the current-induced magnetic field.

Thus, the total energy associated with a transition of an electron with spin  $s$  in direction  $d = \pm 1$  (forward or backward) is then given by:

$$\Delta E = qV + E_{\text{eMChA}} \quad (7)$$

meaning eMChA can either intensify or debilitate the energy bias between two adjacent sites that is originally created by the external voltage.

We can see that three signs are multiplied in equation 6, exactly as in the simplified expression  $(-1)^{scv}$  introduced above, electron spin  $s$  times molecular chirality  $c$  times electron velocity  $v$ . Indeed it is a different expression for the same physics, since  $c$  is proportional to  $\Gamma$  and  $v$

is proportional to  $\tanh\left(\frac{qV}{k_B T}\right)$ . The product between these three parities determines whether a given current direction is favoured or disfavoured for a given electron spin in a given molecular chirality.

## References

1. Gupta, R.; Balo, A.; Garg, R.; Mondal, A. K.; Ghosh, K. B.; Chandra Mondal, P. *Chemical Science* **2024**, 15 (45), 18751–18771. doi:10.1039/d4sc05736h.
2. Bloom, B. P.; Paltiel, Y.; Naaman, R.; Waldeck, D. H. *Chemical Reviews* **2024**, 124 (4), 1950–1991. doi:10.1021/acs.chemrev.3c00661.
3. Alhyder, R.; Lemeshko, M.; Cappellaro, A. *The Journal of Chemical Physics* **2025**, 162 (23), . doi:10.1063/5.0271155.
4. Rikken, G.; Avarvari, N. *The journal of physical chemistry letters* **2023**, 14 (43), 9727–9731.
5. Atzori, M.; Train, C.; Hillard, E. A.; Avarvari, N.; Rikken, G. L. J. A. *Chirality* **2021**, 33 (12), 844–857.
6. Rikken, G. L. J. A.; Raupach, E. *Nature* **1997**, 390 (6659), 493–494.
7. Rikken, G.; Fölling, J.; Wyder, P. *Physical review letters* **2001**, 87 (23), 236602.
8. Ray, K.; Ananthavel, S. P.; Waldeck, D. H.; Naaman, R. *Science* **1999**, 283 (5403), 814–816.
9. Gutiérrez-Finol, G. M.; Rosaleny, L. E.; Camacho-Llovera, A.; Gaita-Ariño, A. *ChemRxiv* **2025**. doi:10.26434/chemrxiv-2025-1118f.
10. Gutiérrez-Finol, G. M.; Zinovjev, K.; Gaita-Ariño, A.; Cardona-Serra, S. **2025**. doi:10.48550/ARXIV.2511.09413.
11. Gutiérrez-Finol, G. M.; Giménez-Santamarina, S.; Hu, Z.; Rosaleny, L. E.; Cardona-Serra, S.; Gaita-Ariño, A. *npj Computational Materials* **2023**, 9 (1), 196.

12. Fransson, J.; Turin, L. *The Journal of Physical Chemistry Letters* **2024**, *15* (24), 6370–6374.
13. Rikken, G. L.; Avarvari, N. *Nature Communications* **2022**, *13* (1), 3564.